Chapter 1
Introduction

1.1 General

The term *fluvial* is commonly used in geophysics and earth sciences to refer to the processes associated with rivers or streams, and the erosions or deposits and morphology created by them. The subject *hydrodynamics* under the curriculum of civil engineering and environmental engineering becomes more diverse including the mechanism of the processes associated with fluvial systems. Fluvial processes comprise the sediment transport and aggradations or degradations of the riverbeds. The flow over a bed formed by the loose sediment exerts a shear stress on the bed. If the stabilizing resistance to the sediment particles is lower than the bed shear stress exerted, the sediment can be mobilized. For each particle size, there is a specific velocity or bed shear stress at which the particles on the bed surface start to move, called the *threshold velocity or threshold shear stress*, respectively. Sediment transport by the stream flows can occur in different modes. Sediment in rivers is transported as *bed load* (coarser fractions which move close to the bed) and/or *suspended load* (finer fractions carried by the flow). There is also a component carried as *wash load* that remains near the free surface of flow. Little is known specifically about the wash load where it comes from or where it goes. Further, during the sediment transport, the riverbed takes different undular features, called the *bedforms*. All these related to sediment transport make the flow in a river rather intricate, as compared to that in a rigid-bed channel. Further, the flow in rivers is locally modified by the embedded obstacles, such as bridge piers, abutments, and pipelines and the hydraulic structures, such as barrages, drops, and sills. The modified flow has enormous erosive potential causing a *local scour* near the obstacles and the hydraulic structures.

A natural river continually picks up sediment from and drops sediment on its bed throughout its course. Where the river flows with high velocity, more sediment is picked up than dropped. In contrast, where the flow is tranquil, more sediment is dropped than picked up. These processes including the formations of bedforms, such as ripples, dunes, and antidunes, determine the complex morphology of a river. In a typical river, the largest carried sediment is of sand and gravel size, but a

S. Dey, *Fluvial Hydrodynamics*, GeoPlanet: Earth and Planetary Sciences,
DOI: 10.1007/978-3-642-19062-9_1, © Springer-Verlag Berlin Heidelberg 2014

larger flood can carry cobbles and even boulders. The amount of sediment carried by a large river is enormous. For instance, the Mississippi in USA annually carries 406×10^6 tons of sediment to the sea, the Hwang Ho in China 796×10^6 tons and the Po in Italy 67×10^6 tons.

The origin of the development of *fluvial hydrodynamics* dates back to the distant past, as people faced the problems due to erosion, sedimentation, and floods. The ancient civilizations particularly in the valleys of Indus, Tigris, Euphrates, Nile, and Hwang Ho rivers used the unlined canals for irrigation. Historical records suggest that about six thousand years ago, marginal embankments were built along the Hwang Ho in China; irrigation canals and flood control structures constructed in Mesopotamia; and one thousand years afterward a masonry dam built across the Nile in Egypt. In India, more than five thousand years ago, the mechanics of sediment transport by stream flows was explained by *sage Vashistha*. During the Renaissance era, famous Italian painter and scientist-cum-engineer *Leonardo da Vinci* made the first empirical studies of streams and their velocity distributions. His notebooks are full of observations that he made on rivers; and they reveal that he understood the principles of sedimentation and erosion. Since then, scientists and engineers have performed a large number of studies on rivers.

The subject *fluvial hydrodynamics*, being important in the fields of civil engineering, environmental engineering, sedimentary geology, and earth sciences, is most often used to know whether erosion or deposition of sediment or even transport of sediment can occur. If so, what are the magnitude of erosion or deposition and the duration or transport rate? Even though enormous efforts have been made by scientists and engineers to resolve various problems related to sediment transport, due to inherent complexities involved in sediment transport processes and difficulties in taking accurate measurements, inadequate landmark breakthroughs have so far been achieved on a sizable number of key problems. As such, the knowledge on such complex problems is still limited to the perceptual state. Therefore, the research on sediment transport should be directed in solving problems, that often arise in practice involving inherent complex phenomena.

Knowledge of sediment transport can be applied extensively in civil engineering such as to plan the extended life of a dam forming a reservoir. Sediment carried by a river deposits into a reservoir formed by a dam developing a reservoir delta. The delta grows with time filling the reservoir to reduce its capacity, and eventually, either the reservoir needs to be dredged or the dam needs to be abandoned. Also an adequate knowledge of the mechanics of sediment transport in a built environment is important for civil and hydraulic engineers. Flow in culverts, over spillways, below pipelines, and around bridge piers/abutments creates scour, which can damage the environment and expose the foundations of the structures being detrimental to them.

Sediment transport, being applied in solving various environmental engineering problems, is important in providing habitat for fish in rivers and other instream organisms, sustaining a hygienic stream ecosystem. On the other hand, when suspended load of sediment is substantial due to human activities, it can cause environmental hazards including the filling up of the channels by siltation.

Geologists, on the other hand, seek inverse solutions for sediment transport relationships to get an idea on the flow depth, velocity, and direction, from the characteristics of the sedimentary rocks and new deposits of sediment particles.

1.2 Scope of this Book

The aim of the science of fluvial hydrodynamics is to understand the behavior of sediment transport in natural streams and to provide a basis for predicting its responses to natural or man-made disturbances. However, in general, the basic problem of flow over a sediment bed can be stated in a rather deceptively simple way: Given the sediment characteristics, flow rate and bed slope; what are the probable flow depth and the sediment transport rate? Even for the simplest case of a two-dimensional flow over a flat bed formed by a uniform sediment size, a general solution can only be presented with estimates involving high degree of uncertainty, as much of the intricacy lies on velocity or turbulent stress distribution over a sediment bed. Advances in measurement technology and progress in understanding of the turbulence phenomena in shear flow within near-bed flow region inspire recent research trend that may append to a more satisfactory response to the basic questions. Moreover, this topic has attracted the attention not only of engineers but also of earth scientists, with potentially constructive results and contributions being published in leading journals, reports, and monographs not essentially familiar to the hydraulic engineering communities.

The objective of this book is therefore to develop a sound qualitative and quantitative basis of knowledge of the subject. This book is rather different from a typical engineering treatment of open-channel flow in its larger emphasis on fluvial streams and their interactions with structures, such as, bridge piers and abutments, bed sills. It also differs from a general earth science-oriented treatment in its extended emphasis on the analyses based on the physics of turbulent flow and its customary applications developed for engineering practices. To be useful, a special attempt is made in this book to include the new important research results on sediment transport achieved over the past years. It seems to be a demand, as over decades, there have been inadequate efforts in incorporating of new developments that help to predict sediment transport processes more accurately and are also helpful in field situations not so far included in the traditional textbooks.

1.3 Coverage of this Book

The topics of this book include hydrodynamic principles and turbulence characteristics related to open-channel flow, mechanics of sediment transport, and local scour phenomena including application examples in fluvial hydrodynamics. It is organized into eleven chapters. They are as follows:

This chapter provides an introduction to the fluvial hydrodynamics, scope and outline of this book, and the properties of fluid and sediment. Chapter 2 introduces the fundamental theories of hydrodynamics in the context of open-channel flow. Chapter 3 presents the turbulence characteristics in flow over a sediment bed. It includes most of the modern development of turbulent flow, such as bursting phenomenon, double averaging of heterogeneous flow over gravel-beds. Chapter 4 is devoted to the theories of the initiation of sediment motion. It encompasses different concepts of sediment threshold and their theoretical and empirical developments. Chapter 5 describes the concepts, theories, and empirical formulations of bed load transport and saltation, while Chaps. 6 and 7 illustrate those of suspended and total load transports, respectively. Chapter 8 demonstrates different types of bedforms and their mechanism of formation and resistant to flow. Chapter 9 describes the natural fluvial processes toward meanderings and braiding. Chapter 10 outlines comprehensive information on local scour within channel contractions, downstream of structures, below horizontal pipelines, at bridge piers and abutments, and scour countermeasures. Chapter 11 is designed to deal with the issue to describe dimensional analysis, modeling, and similitude of sediment transport and scour problems.

The general feature of all the chapters is shaped by the fundamentals, such as the definitions of the phenomena and the involved parameters as well as a series of methodologies, starting from the earlier developments and ending to the latest ones.

In the end of each chapter, bibliographical references are given.

1.4 Physical Properties of Fluid and Sediment

Following properties of fluid and sediment are of general importance to study the fluvial hydrodynamics. For the convenience, typical values, SI units, and dimensions in MLT system (also see Chap. 11) are given.

1.4.1 Mass Densities of Fluid and Sediment

The *mass density* ρ of a fluid is defined as its mass per unit volume. The mass density at a point is determined by considering the mass dm of a small volume dV surrounding the point. As dV becomes a magnitude ε^3, where ε is the small linear distance but larger than the mean distance between molecules, the mass density at a point is given by

$$\rho = \lim_{\mathrm{d}V \to \varepsilon^3} \frac{\mathrm{d}m}{\mathrm{d}V} \tag{1.1}$$

Similarly, the *mass density* ρ_s of a sediment sample is defined as its mass per unit solid volume (without void). In case of a single particle, the mass and the volume refer to those of that particle. However, the *submerged density* of a sediment sample denoted by $\Delta\rho$ is $\rho_s - \rho$.

Its unit is kg m^{-3} and dimension ML^{-3}. Typical value of ρ for water is 10^3 kg m^{-3} at standard atmospheric pressure of 1.013×10^5 Pa (or 0.76 m height of mercury in a barometer) and temperature of 4 °C, while typical value of ρ_s for a quartz sand sample is 2.65×10^3 kg m^{-3}. Mass density of water varies with temperature. The dependency of the mass density of water on temperature is given by $\rho = 10^3 - 6.5 \times 10^{-3}(t - 4)$ kg m^{-3}, where t is the temperature in °C.

1.4.2 Specific Weights of Fluid and Sediment

The *specific weight* γ of a fluid is defined as its weight per unit volume. Since weight is dependent on acceleration due to gravity g, the specific weight of a fluid varies from place to place. It is therefore related to the mass density as

$$\gamma = \rho g \tag{1.2}$$

Similarly, the *specific weight* γ_s of a sediment sample is defined as its weight per unit solid volume. In case of a single particle, the weight and the volume refer to those of that particle. However, the *submerged specific weight* of a sediment sample denoted by $\Delta\gamma$ is $\gamma_s - \gamma$.

Its unit is N m^{-3} and dimension ML^{-2} T^{-2}. Typical value of γ for water is 9.81×10^3 N m^{-3} at a place where g is 9.81 m s^{-2}, while typical value of γ_s for a quartz sand sample is $2.65 \times 9.81 \times 10^3$ N m^{-3}.

1.4.3 Relative Densities of Fluid and Sediment

The *relative density* s_f of a fluid is defined as the ratio of the mass density of fluid to the mass density of water at 4 °C.

Similarly, the *relative density* s of a sediment sample is defined as the ratio of the mass density of sediment to the mass density of water at 4 °C. However, the *submerged relative density* of a sediment sample denoted by Δ is $s - s_f$.

The relative density has no unit being represented by a number. Its dimension is M^0 L^0 T^0 (=1). Typical values of s_f for water and s for a quartz sand sample are 1 and 2.65, respectively.

1.4.4 Viscosity of Fluid

By definition, *fluid* is a substance that deforms continuously under the action of shear force, however, small it may be. Shear force within successive layers of fluid parallel to the boundary is the consequence of the fluid flow having differential velocities of the layers. The velocities of the layers increase away from the boundary, while the fluid particles in contact with the boundary have the same velocity as the boundary, called the *no-slip condition*. For the fluids obeying the *Newton's law of viscosity*, the shear stress τ being proportional to the velocity gradient therefore is given by

$$\tau = \mu \frac{\mathrm{d}u}{\mathrm{d}z} \tag{1.3}$$

where μ is the *coefficient of dynamic viscosity* and u is the velocity in x-direction (that is the streamwise direction) at a normal distance z from the boundary.

Rearranging Eq. (1.3), the *coefficient of dynamic viscosity* (in short, also called *dynamic viscosity*) μ is defined as the shear stress (that is the shear force per unit area) required to drag one layer of fluid with a unit velocity past another layer at a unit distance apart. Its unit is Pa s and dimension $\mathrm{ML^{-1}\,T^{-1}}$. Note that the dynamic viscosity is often measured in poise (P), which equals 0.1 Pa s. Typical value of μ for water is approximately 10^{-3} Pa s at 20 °C.

Note that the *laminar flow* (also called *viscous flow*) is represented by a series of parallel layers sliding over another without any exchange of mass between the layers. In turbulent flow, however, the mixing between the layers takes place, and the shear stress τ is given by

$$\tau = (\mu + \varepsilon_t \rho) \frac{\mathrm{d}\bar{u}}{\mathrm{d}z} \tag{1.4}$$

where ε_t is the *coefficient of eddy viscosity* or *turbulent diffusivity* and $\bar{u}$ is the time-averaged velocity in x-direction at a normal distance z from the boundary. Details of turbulent diffusivity and its role are given in Chaps. 3 and 6.

Removing the mass term from the dynamic viscosity expression by dividing it by the mass density ρ of fluid, the *coefficient of kinematic viscosity* (in short, also called *kinematic viscosity*) υ is obtained. Hence, it is defined as the ratio of dynamic viscosity to mass density:

$$\upsilon = \frac{\mu}{\rho} \tag{1.5}$$

Its unit is $\mathrm{m^2\,s^{-1}}$ and dimension $\mathrm{L^2\,T^{-1}}$. Note that the kinematic viscosity is often measured in stokes (St), which equals $10^{-4}\ \mathrm{m^2\,s^{-1}}$. Typical value of υ for water is approximately $10^{-6}\ \mathrm{m^2\,s^{-1}}$ at 20 °C.

Viscosity is dependent on temperature, but independent of pressure. The dependency of kinematic viscosity on temperature of river water is given by $\upsilon = [1.14 - 3.1 \times 10^{-2}(t - 15) + 6.8 \times 10^{-4}(t - 15)^2] \times 10^{-6}$ m^2 s^{-1}, where t is in °C (Julien 1998).

1.4.5 Size of a Sediment Particle

Particle size is the most important parameter to deal with sediment transport processes. The mode of sediment transport and the corresponding mechanism are partially dependent on the particle size to be transported. The size of a sediment particle can be represented by a number of ways: *Nominal diameter*, *area diameter*, *sieve diameter*, *fall diameter*, and *sedimentation diameter*. The SI units are used to represent the sediment size in m. However, the sediment size is also expressed in mm, micron (1 μm = 10^{-3} mm) and logarithmic units Φ.

Nominal diameter, d_n: It is the diameter of a sphere having the same volume as that of a given sediment particle:

$$d_n = \left(\frac{6V}{\pi}\right)^{1/3} \tag{1.6}$$

where V is the volume of sediment particle. The approximate volume can be estimated considering a sediment particle as an ellipsoid as $V \approx \pi a_1 a_2 a_3/6$, where a_1, a_2, and a_3 are the longest, intermediate, and shortest lengths along mutually perpendicular axes of a Cartesian coordinate system.

Area diameter, d_a: It is the diameter of a sphere having the same surface area as that of a given sediment particle:

$$d_a = \left(\frac{S}{\pi}\right)^{0.5} \tag{1.7}$$

where S is the total surface area of sediment particle. The area diameter is usually used to characterize the flat-shaped particles (Mehta et al. 1980; Dey 2003).

Sieve diameter, d: It is the diameter of a sphere equaling the side length of a square sieve opening through which a given sediment particle can just pass. For sediment sizes (0.2–20 mm) of natural streambeds, sieve diameter is approximately equaling $0.9d_n$ (US Interagency Committee 1957).

Fall diameter, d_t: It is the diameter of a sphere having a relative density of 2.65 and a same terminal fall velocity as that of a given sediment particle in quiescent, pure water at 4 °C.

Sedimentation diameter, d_w: It is the diameter of a sphere having equal terminal fall velocity and relative density as those of a given sediment particle in the same sedimentation fluid under the same atmospheric pressure and temperature.

Table 1.1 Grade scale of sediment size

Class	Size range	
	mm	Φ units
Very large boulder	$4{,}000 \geq d > 2{,}000$	
Large boulder	$2{,}000 \geq d > 1{,}000$	
Medium boulder	$1{,}000 \geq d > 500$	
Small boulder	$500 \geq d > 250$	$-9 \leq \Phi < -8$
Large cobble	$250 \geq d > 130$	$-8 \leq \Phi < -7$
Small cobble	$130 \geq d > 64$	$-7 \leq \Phi < -6$
Very coarse gravel	$64 \geq d > 32$	$-6 \leq \Phi < -5$
Coarse gravel	$32 \geq d > 16$	$-5 \leq \Phi < -4$
Medium gravel	$16 \geq d > 8$	$-4 \leq \Phi < -3$
Fine gravel	$8 \geq d > 4$	$-3 \leq \Phi < -2$
Very fine gravel	$4 \geq d > 2$	$-2 \leq \Phi < -1$
Very coarse sand	$2 \geq d > 1$	$-1 \leq \Phi < 0$
Coarse sand	$1 \geq d > 0.5$	$0 \leq \Phi < 1$
Medium sand	$0.5 \geq d > 0.25$	$1 \leq \Phi < 2$
Fine sand	$0.25 \geq d > 0.125$	$2 \leq \Phi < 3$
Very fine sand	$0.125 \geq d > 0.062$	$3 \leq \Phi < 4$
Coarse silt	$0.062 \geq d > 0.031$	$4 \leq \Phi < 5$
Medium silt	$0.031 \geq d > 0.016$	$5 \leq \Phi < 6$
Fine silt	$0.016 \geq d > 8 \times 10^{-3}$	$6 \leq \Phi < 7$
Very fine silt	$8 \times 10^{-3} \geq d > 4 \times 10^{-3}$	$7 \leq \Phi < 8$
Coarse clay	$4 \times 10^{-3} \geq d > 2 \times 10^{-3}$	$8 \leq \Phi < 9$
Medium clay	$2 \times 10^{-3} \geq d > 10^{-3}$	
Fine clay	$10^{-3} \geq d > 5 \times 10^{-4}$	
Very fine clay	$5 \times 10^{-4} \geq d > 2.4 \times 10^{-4}$	

Φ *units*: In order to facilitate the sediment size representation by a nondimensional number, another standard way to specify particle sizes is the Φ scale, in which $d = 2^{-\Phi}$ (Krumbein and Sloss 1963). Taking the logarithmic of both sides, Φ units for given sediment sizes are determined as

$$\Phi = -\log_2 d = -\frac{\log_{10} d}{\log_{10} 2} \tag{1.8}$$

where d is in mm. For example, $\Phi(d = 4 \text{ mm}) = -2$. From Eq. (1.8), it implies that $\Phi(d = 1 \text{ mm}) = 0$.

Table 1.1 furnishes the sediment size classification based on grade scale, as recommended by the subcommittee on sediment terminology of the AGU (Lane 1947), which is widely used by the hydraulicians and geologists.

1.4.6 Shape of a Sediment Particle

The shape of a given sediment particle refers to the general geometric form apart from its size and material composition. In sediment analysis, one of the most relevant shape parameters is *sphericity*, S_c. According to Wadell (1932), the sphericity is defined as the ratio of the surface area of a sphere of the same volume as that of a given sediment particle to the actual surface area of the particle. The sphericity basically characterizes the motion of a settling particle relative to the fluid. As the actual surface area of a small particle is rather difficult to obtain, Wadell redefined the sphericity as

$$S_c = \left(\frac{V}{V_c}\right)^{1/3} \tag{1.9}$$

where V_c is the volume of circumscribing sphere. However, the sphericity can also be approximated as $S_c \approx d_n/a_1$. Also, Krumbein (1941) expressed the sphericity as

$$S_c = \left(\frac{a_2 a_3}{a_1^2}\right)^{1/3} \tag{1.10}$$

On the other hand, *roundness* is defined as the average radius of curvature of several edges of a given sediment particle to the radius of a circle inscribed in the maximum projected area of the particle. Unlike sphericity, roundness has been found to be a trivial parameter in the hydrodynamics of sediment transport.

Importantly, the irregular-shaped particles are usually defined by the *Corey shape factor* S_p (Vanoni 1977) as

$$S_p = \frac{a_3}{(a_1 a_2)^{0.5}} \tag{1.11}$$

The Corey shape factor which is always less than unity is typically 0.7 for naturally worn particles. The main drawback of using Corey shape factor is that it does not take into account the distribution of the surface area and the volume of the particle. For example, a cube and a sphere have the same shape factor S_p being unity. Nevertheless, the hydrodynamic characteristics, such as drag and lift forces, induced on a cubical particle and a spherical particle are different. To overcome this difficulty, Alger and Simons (1968) proposed a *shape parameter* S_{sp} that is given by

$$S_{sp} = S_p \frac{d_a}{d_n} \tag{1.12}$$

According to Heywood (1938), another shape description can be given as *volume coefficient* k_v, which is the ratio of the volume of a given sediment particle to the cube of the diameter D of circle containing the projected area of the particle onto the plane parallel to a_1a_2-plane. Hence, $k_v = V/D^3$. For natural sediments, k_v is approximately 0.3. He also defined *surface coefficient* k_c as $k_c = S/D^2$

1.5 Properties of Sediment Mixture

1.5.1 Size Distribution

The fluvial sediment is usually composed of mixture of particles of various sizes. The size distribution of a sediment mixture can be measured by the sieve analysis. Typical results of the sieve analysis of adequate quantity of representative sediment sample are presented in the form of a *frequency histogram* (or a *frequency curve*) (Fig. 1.1a) and a *cumulative frequency curve* (Fig. 1.1b). The cumulative frequency curve is also commonly known as *particle size distribution curve*. In the frequency curve (Fig. 1.1a), the abscissa represents the particle size d class intervals in logarithmic scale and the ordinate the percentage concentration (by weight) of the total sample contained in the corresponding intervals of the particle size class. On the other hand, the particle size distribution curve represents the variation of the percentage (by weight) of sediment finer (in the ordinate) than a given sediment size d (in the abscissa using logarithmic scale) in the total sample, as shown in (Fig. 1.1b).

Very often, the size distribution of natural well-graded sediments follows the lognormal probability curve when plotted. The probability distribution $f(d)$ and the cumulative distribution $F(d)$ can be approximated by the lognormal and the error function distributions, respectively, as given by the following expressions [see Fredsøe and Deigaard (1992)]:

$$\begin{aligned} f(d) &= \frac{1}{d\sqrt{2\pi}\ln\sigma_g}\exp\left\{-\frac{1}{2}\left[\frac{\ln(d/d_{50})}{\ln\sigma_g}\right]^2\right\}, \\ F(d) &= \frac{1}{2}\left\{1+\operatorname{erf}\left[\frac{1}{\sqrt{2}}\cdot\frac{\ln(d/d_{50})}{\ln\ \sigma_g}\right]\right\} \end{aligned} \tag{1.13}$$

where σ_g is the geometric standard deviation of particle size distribution and d_{50} is the median particle diameter or 50 % finer particle size, which can be obtained from the particle size distribution curve (Fig. 1.1b). Besides the lognormal distribution, natural sediments may also have a bimodal distribution that displays two distinct peaks in a frequency distribution curve characterizing each peak as the mode of the distribution. Nonuniform sediments with a distinctive finer and coarser size of sediment mixture can have bimodal distribution.

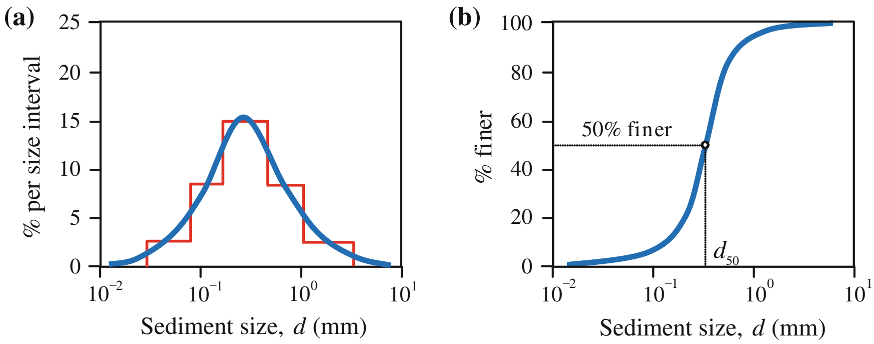

Fig. 1.1 **a** Typical frequency histogram and frequency distribution curve and **b** typical cumulative frequency distribution or particle size distribution curve

The *geometric standard deviation* σ_g is an important parameter used to determine the nonuniformity of a sediment mixture. It is expressed as

$$\sigma_g = \frac{d_{84.1}}{d_{50}} = \frac{d_{50}}{d_{15.9}} = \left(\frac{d_{84.1}}{d_{15.9}}\right)^{0.5} \tag{1.14}$$

where $d_{84.1}$ and $d_{15.9}$ are 84.1 and 15.9 % finer diameters, respectively. For a given particle size distribution, if $\sigma_g \leq 1.4$, then the sediment is considered to be uniform; otherwise, the sediment is nonuniform (Dey and Sarkar 2006). The *geometric mean size* d_g is the square root of the product of $d_{84.1}$ and $d_{15.9}$.

$$d_g = (d_{84.1} d_{15.9})^{0.5} \tag{1.15}$$

Apart from the geometric standard deviation, the *gradation coefficient* G is in use. It is given by

$$G = \frac{1}{2}\left(\frac{d_{84.1}}{d_{50}} + \frac{d_{50}}{d_{15.9}}\right) \tag{1.16}$$

In addition, Kramer (1935) proposed a *uniformity parameter* M that is defined as the ratio of the median sizes of the two portions in the particle size distribution curve separated by the median particle size d_{50}:

$$M = \frac{\sum_{i=0}^{i=50} p_i d_i}{\sum_{i=50}^{i=100} p_i d_i} \tag{1.17}$$

where i is the cumulative percentage of sediment finer than d_i and p_i is the fraction of each size class in percentage. Kramer's uniformity parameter $M = 1$ for uniform sediment and $M < 1$ for nonuniform sediment.

The relationship between d_i and Φ_i is therefore expressed as

$$\Phi_i = -\frac{\log_{10} d_i}{\log_{10} 2} \tag{1.18}$$

1.5.2 Porosity, Void Ratio, Dry Mass Density, and Dry Specific Weight

The *porosity* ρ_0 of a sediment mixture is defined as the volume of void per unit total volume. If the volume of void is V_v and the volume of solid is V_s, then the porosity is given by

$$\rho_0 = \frac{V_\mathrm{v}}{V_\mathrm{v} + V_\mathrm{s}} \tag{1.19}$$

Komura (1963) gave an empirical relationship for the porosity of unconsolidated saturated sediment as

$$\rho_0 = 0.245 + \frac{0.14}{d_{50}^{0.21}} \tag{1.20}$$

where d_{50} is in mm. Using the laboratory experimental and field data, Wu and Wang (2006) modified Komura's relationship as

$$\rho_0 = 0.13 + \frac{0.21}{(0.002 + d_{50})^{0.21}} \tag{1.21}$$

The *void ratio* e of a sediment mixture is defined as the volume of void per unit volume of solid; and hence, it can be related with the porosity as

$$e = \frac{V_\mathrm{v}}{V_\mathrm{s}} = \frac{\rho_0}{1 - \rho_0} \tag{1.22}$$

The *dry mass density* ρ_d and the *dry specific weight* γ_d of a sediment mixture are defined as the mass and the weight of solid per unit total volume, respectively. They are expressed in terms of porosity as

$$\rho_\mathrm{d} = \rho_\mathrm{s}(1 - \rho_0), \quad \gamma_\mathrm{d} = \gamma_\mathrm{s}(1 - \rho_0) \tag{1.23}$$

1.5.3 Angle of Repose

The *angle of repose* ϕ (or more precisely, the *critical angle of repose*) is the steepest angle of descent of the slope with respect to the horizontal plane when the sediment particles submerged in water are on the verge of sliding on the sloping surface of a sediment heap. The angle of repose therefore corresponds to a so-called sediment avalanche. The angle of repose is approximately equal to the angle of internal friction at the contacts of the sediment particles. Hence, ϕ approximately equals arctan μ_d, where μ_d is the static Coulomb friction coefficient. Note that the force, in addition to inertia, opposing the motion of noncohesive sediments at contacts is friction. The friction coefficient μ_d is therefore described as the ability of a particle to resist motion (sliding) relative to its submerged gravity component normal to the sliding; it therefore represents the ratio of the tangential resistive force to the downward normal force.

In mechanics of sediment transport, the angle of repose is assumed to be equivalent to the pivoting angle ϕ of the superimposed particle resting over the bed particles at the point of contact P over which it can move (Fig. 1.2). It is evident that the superimposed particle can roll over either the points of contact of the valley formed by the two bed particles or the single point of contact of a bed particle, depending on the arrangement or the orientation of bed particles and according to the direction of superimposed particle tending to move. Importantly, the angle of repose varies significantly with the nonuniformity of sediments, while for uniform sediments, the values of ϕ lie in between 28 and 32°.

Zhang et al. (1989) proposed an empirical relationship for the angle of repose of noncohesive sediment with sediment size as

$$\phi = 32.5 + 1.27 d_{50} \tag{1.24}$$

where ϕ is in deg and d_{50} in mm. Equation (1.24) is applicable for the sediment size range $0.2 \leq d_{50} \leq 4.4$ mm.

For a simple case of spherical particles, Fig. 1.2 clearly depicts that the angle of repose varies with the ratio of the size of superimposed spherical particle to that of bed particles over which it rests. Ippen and Eagleson (1955) gave an equation of angle of repose for spherical particles as

$$\tan\phi = 0.866\left[\left(\frac{d}{k_s}\right)^2 + 2\left(\frac{d}{k_s}\right) - \frac{1}{3}\right]^{-0.5} \tag{1.25}$$

where d is the sediment particle diameter and k_s is the bed particle size or bed roughness height. Li and Komar (1986) showed that the angle of repose decreases with an increase in d/k_s. The relationship, which is applicable for $0.3 < d/k_s < 3$, is

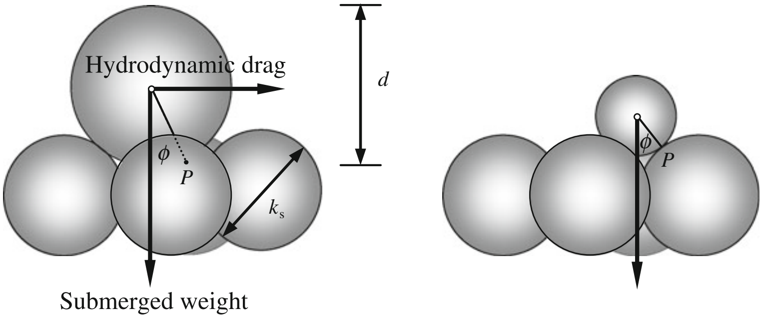

Fig. 1.2 Schematic of pivoting angles of superimposed sediment particles relative to bed particles

Table 1.2 Values α and β as proposed by Li and Komar (1986)

Shape	α	β
Sphere	51.3	0.33
Ellipsoidal gravels	31.9	0.36
Angular gravels	36.3	0.72 for $d/k_s > 1$
	36.3	0.55 for $d/k_s < 1$

$$\phi = \alpha \left(\frac{d}{k_s} \right)^{-\beta} \tag{1.26}$$

where α and β are coefficient and exponent dependent on the shape of the particles, respectively. Li and Komar (1986) determined the values of α and β for spheres, ellipsoidal, and angular gravels, as given in Table 1.2.

It is pertinent to mention that in natural conditions, the values of angle of repose vary to a wide range that it is not easy to determine in field situations.

1.6 Properties of Fluid and Suspended Sediment Mixture

Figure 1.3 shows a schematic of sediment suspension in fluid, called *fluid–sediment mixture*, consisting of a volume of sediment V_s and a volume of fluid V_f. Note that the volume of fluid here equals the volume of void, that is $V_f = V_v$. The *sediment concentration* C by volume is defined as

$$C = \frac{V_s}{V_f + V_s} \tag{1.27}$$

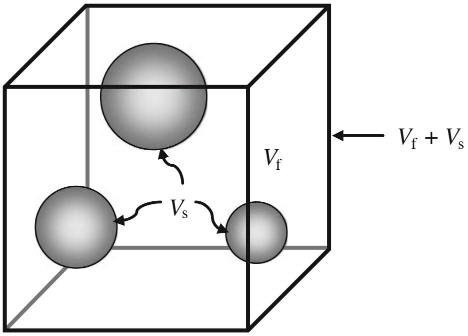

Fig. 1.3 Schematic of sediment suspension in fluid

On the other hand, the *sediment concentration c* by mass is defined as

$$c = \frac{\rho_s V_s}{\rho V_f + \rho_s V_s} = \frac{(\rho_s/\rho)C}{1 + [(\rho_s/\rho) - 1]C} \tag{1.28}$$

Equation (1.28) remains same for the sediment concentration by weight, since the equation is transformed to weight of the quantities by multiplying the numerator and the denominator with the same value of g. In case of water as a fluid, Eq. (1.28) becomes $c = sV_s/(V_f + sV_s) = sC/(1 + \Delta C)$, where $\Delta = s - 1$. Sediment concentration is usually expressed in parts per million (ppm) by mass or weight, that is $10^6 c$. However, sediment concentration is also expressed in mass per unit volume of concentration, $\rho_s C$, or in weight per unit volume of concentration, $\gamma_s C$. The *mass density of fluid–sediment mixture* ρ_m is expressed as

$$\rho_m = \rho + (\rho_s - \rho)C \tag{1.29}$$

The *specific weight of fluid–sediment mixture* γ_m is

$$\gamma_m = \gamma + (\gamma_s - \gamma)C = \rho_m g \tag{1.30}$$

The *kinematic viscosity of fluid–sediment mixture* υ_m is

$$\upsilon_m = \frac{\mu_m}{\rho_m} \tag{1.31}$$

where μ_m is the dynamic viscosity of fluid–sediment mixture. Based on the experimental results for $0.2 \le C \le 0.6$, Bagnold (1954) formulated the dynamic viscosity of water–sediment mixture as

$$\mu_m = \mu \left[1 + \frac{1}{(0.74/C)^{1/3} - 1}\right]\left[1 + \frac{0.5}{(0.74/C)^{1/3} - 1}\right] \tag{1.32}$$

Here, μ is the dynamic viscosity of a clear water. Also, an empirical relationship for μ_m was given by Lee (1969) as

$$\mu_m = \mu(1 - C)^{-(2.5+1.9C+7.7C^2)} \tag{1.33}$$

1.7 Terminal Fall Velocity of Sediment in Fluid

1.7.1 Terminal Fall Velocity of a Spherical Particle

The gravitational fall velocity of sediment is one of the key parameters in sediment transport, especially when sediment suspension is the dominant process. It acts as a restoring force against turbulent entraining force acting on the particle. Knowledge on fall velocity of a particle is thus important. In sediment transport, although natural sediment is seldom spherical, the fall velocity of a rigid sphere is usually used as an approximation in predicting fall velocity of a sediment particle in natural streams.

In hydrodynamics, a particle falls at its terminal velocity if its velocity is constant due to the drag exerted by the fluid through which it falls. As a falling particle accelerates under the gravity, the drag force acting on the particle increases with an increase in velocity, causing the acceleration of the particle or in turn, the inertia force acting on the particle to reduce. At the point, the particle ceases to accelerate and continues falling at a constant velocity, called the *terminal fall velocity* or *settling velocity*. A free-falling particle therefore attains its terminal fall velocity w_s when the submerged gravity force F_G of the particle equals the upward drag force F_D, as shown in Fig. 1.4.

For a spherical particle falling with a terminal fall velocity w_s in a column of water, the following equation is thus obtained:

$$\underbrace{\Delta\rho g \frac{\pi}{6} d^3}_{F_G} = \underbrace{C_D \frac{\rho}{2} w_s^2 \frac{\pi}{4} d^2}_{F_D} \Rightarrow w_s = \left(\frac{4}{3} \cdot \frac{\Delta g d}{C_D}\right)^{0.5} \tag{1.34}$$

where Δ is $s - 1$, ρ is the mass density of water, d is the diameter of falling particle, and C_D is the drag coefficient.

Neglecting all inertia terms, Stokes (1851) analyzed the Navier–Stokes equations for laminar flow range of particle Reynolds number R_e (= $w_s d/\upsilon$) < 1 aided by

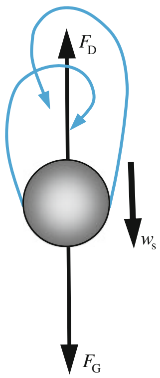

Fig. 1.4 Schematic of a sphere falling in a static fluid with a terminal fall velocity w_s

a stream function to derive a solution for the drag as $F_D = 3\pi\mu d w_s$ (see Sect. 2.8) that yields

$$C_D = \frac{24}{R_e} \tag{1.35}$$

Oseen (1927) included some inertia terms in solving the Navier–Stokes equations to obtain the drag coefficient as

$$C_D = \frac{24}{R_e}\left(1 + \frac{3}{16}R_e\right) \tag{1.36}$$

Afterward Goldstein (1929), who gave an extended solution of Oseen's approximation, determined the drag coefficient as

$$C_D = \frac{24}{R_e}\left(1 + \frac{3}{16}R_e - \frac{19}{1280}R_e^2 + \frac{71}{20480}R_e^3 + \cdots\right) \tag{1.37}$$

Equation (1.37) is applicable for $R_e \le 2$. For $R_e > 2$, the drag coefficient that could not be found theoretically had to be determined empirically. Schiller and Naumann (1933) used experimental data for $R_e < 800$ to fit a curve with the following relationship:

$$C_D = \frac{24}{R_e}\left(1 + 0.15R_e^{0.687}\right) \tag{1.38}$$

Rouse (1938) used the available experimental data to prepare a $C_D(R_e)$ curve for the estimation of terminal fall velocity of a sphere, as shown in Fig. 1.5. Figure 1.5 also provides a good comparison of the variation of C_D with R_e obtained from the formulas given by different investigators. Importantly, in turbulent settling region

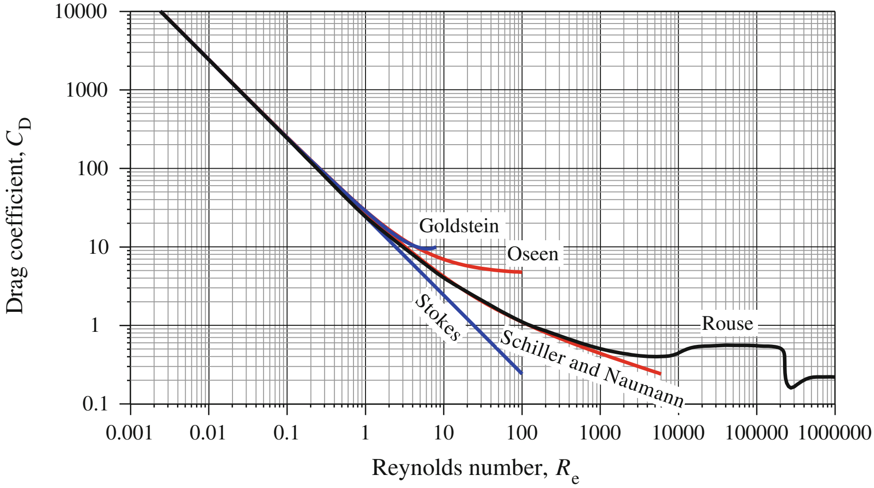

Fig. 1.5 Drag coefficient as a function of particle Reynolds number for sphere

of particle Reynolds number, $R_e > 10^3$, the drag coefficient is not only poorly correlated with the particle Reynolds number R_e but also invariant of it for certain ranges of R_e.

1.7.2 Terminal Fall Velocity of Sediment Particles

Rubey (1933) was the first to introduce a formula for the determination of terminal fall velocities of gravel, sand, and silt particles. Since then, many investigators put forward number of semitheoretical and empirical relationships for the terminal fall velocity of sediment particles. Generally, the drag coefficient, according to Cheng (1997), can be generalized as

$$C_D = \left[\left(\frac{P}{R_e}\right)^{1/m} + Q^{1/m}\right]^m \tag{1.39}$$

where P and Q are the coefficients and m is an exponent. The particle Reynolds number R_e is estimated by using nominal diameter d_n of sediment particles, as $R_e = w_s d_n / \upsilon$. The nominal diameter is approximated as $d_n = d/0.9$, where d is the median sieve diameter of sediment. Using Eq. (1.39), the expression for terminal fall velocity is obtained from Eq. (1.34) (Wu and Wang 2006):

Table 1.3 Values P, Q, and m

References	P	Q	m
Rubey (1933)	24 (for $d_n \le 1$ mm) and 0 (for $d_n > 1$ mm)	2.1	1
Zhang (1961)	34	1.2	1
Zanke (1977)	24 (for $d_n \le 1$ mm) and 0 (for $d_n > 1$ mm)	1.1	1
Raudkivi (1990)	32	1.2	1
Fredsøe and Deigaard (1992)	36	1.4	1
Julien (1998)	24	1.5	1
Cheng (1997)	32	1	1.5
Soulsby (1997)	26.4	1.27	1
She et al. (2005)	35	1.56	1
Wu and Wang (2006)	53.5 exp(–0.65S_p)	5.65 exp(–2.5S_p)	$0.7 + 0.9S_p$
Camenen (2007)	24.6	0.96	1.53

Table 1.4 Formulas given by Hallermeier (1981), Chang and Liou (2001) and Guo (2002)

References	Formula	Range of D_*
Hallermeier (1981)	$w_{sc} = \frac{\upsilon}{d_n} \cdot \frac{D_*^3}{18}$	$D_* \le 3.42$
	$w_{sc} = \frac{\upsilon}{d_n} \cdot \frac{D_*^{2.1}}{6}$	$3.42 < D_* \le 21.54$
	$w_{sc} = 1.05 \frac{\upsilon}{d_n} D_*^{1.5}$	$D_* > 21.54$
Chang and Liou (2001)	$w_{sc} = 1.68 \frac{\upsilon}{d_n} \cdot \frac{D_*^{1.389}}{1 + 30.22 D_*^{-1.611}}$	–
Guo (2002)	$w_{sc} = \frac{\upsilon}{d_n} \cdot \frac{D_*^3}{24 + 0.866 D_*^{1.5}}$	–

$$w_s = \frac{P}{Q} \cdot \frac{\upsilon}{d_n} \left[\sqrt{\frac{1}{4} + \left(\frac{4Q}{3P^2} D_*^3 \right)^{1/m}} - \frac{1}{2} \right]^m \quad \wedge \quad D_* = d_n \left(\frac{\Delta g}{\upsilon^2} \right)^{1/3} \tag{1.40}$$

where D_* is the nondimensional particle parameter.

Table 1.3 furnishes the values of P, Q, and m obtained from the formulas given by different investigators for naturally worn sediment particles with shape factor $S_p \approx 0.7$.

In addition, Hallermeier (1981), Chang and Liou (2001), and Guo (2002) put forward the expressions for $w_s(D_*)$, which could not be arranged in the form given by Eqs. (1.39) and (1.40). For natural sediment particles, the formulas are given in Table 1.4.

A number of relationships for terminal fall velocity for the case of natural sediment particles are found in the literature. Dietrich (1982) analyzed the experimental data and obtained a formula as

$$w_s = \frac{\upsilon}{d_n} 10^{-c_1 + c_2 \log D_* - c_3 (\log D_*)^2 - c_4 (\log D_*)^3 + c_5 (\log D_*)^4} \tag{1.41}$$

where $c_1 = 1.25572$, $c_2 = 2.92944$, $c_3 = 0.29445$, $c_4 = 0.05175$, and $c_5 = 0.01512$.

Another formula proposed by Ahrens (2000) can be given in terms of aforementioned variables as

$$w_s = \frac{\upsilon}{d_n} \left\{ 0.055 D_*^3 \tanh\left[\frac{12}{D_*^{1.77}} \exp(-4 \times 10^{-4} D_*^3) \right] + 1.06 D_*^{1.5} \tanh\left[0.016 D_*^{1.5} \exp\left(-\frac{120}{D_*^3} \right) \right] \right\} \tag{1.42}$$

In an attempt to obtain a more realistic relationship, Jiménez and Madsen (2003) developed a formula by fitting the relatively long expression given by Dietrich (1982). It is

$$W_* = \left(0.954 + \frac{20.48}{S_*} \right)^{-1} \quad \wedge \quad W_* = \frac{w_s}{(\Delta g d_n)^{0.5}} \quad \vee \quad S_* = d_n \frac{(\Delta g d_n)^{0.5}}{\upsilon} \tag{1.43}$$

where W_* is the nondimensional terminal fall velocity and S_* is another nondimensional particle parameter.

Experiments evidenced that in water with dense sediment suspension, the flow around adjacent settling particles induces a greater drag, as compared to that in a clear water. It is known as *hindered settling effect* that results in a terminal fall velocity w_{sc} in a suspended sediment water (sediment-laden water) to reduce from that in a clear water. According to Richardson and Zaki (1954), the terminal fall velocity (or hindered fall velocity) w_{sc} in water with suspended sediment concentration C can be determined by

$$w_{sc} = w_s (1 - C)^n \tag{1.44}$$

where w_s is the terminal fall velocity in a clear water and n is an empirical exponent varying from 4.9 to 2.3 for R_e increasing from 0.1 to 10^3. However, the exponent n is approximately 4 for the particle sizes ranging from 0.05 to 0.5 mm.

Oliver (1961) conducted experiments on terminal fall velocity in water with suspended sediment. He used the data of his experiments and those of McNown and Lin (1952) to propose a formula:

$$w_{sc} = w_s (1 - 2.15C)(1 - 0.75C^{0.33}) \tag{1.45}$$

Sha (1965) proposed a formula applicable for fine sediment $d_{50} \leq 0.01$ mm:

$$w_{sc} = w_s \left(1 - \frac{C}{2d_{50}^{0.5}}\right)^3 \tag{1.46}$$

Soulsby (1997) proposed a formula for the hindered fall velocity in a dense sediment suspension. In his formula (see Table 1.3), a simple change in the values of P and Q due to C is required for the estimation of w_{sc} as given below:

$$P = \frac{26}{(1-C)^{4.7}}, \quad Q = \frac{1.3}{(1-C)^{4.7}} \tag{1.47}$$

Although the empirical formulas summarized here would be adequate for the approximate estimations required by engineers, an accurate estimation of the terminal fall velocity for sediment particles is rather far from being resolved. Nevertheless, the formula that includes a shape factor given by Wu and Wang (2006) seems to be more complete.

1.8 Examples

Example 1.1 A sieve analysis of the riverbed sediment weighing 31.4 N is done. The relative density of sediment is measured as 2.65. The particle size distribution is given in the following table:

Size fraction (mm)	Weight retained (N)	Size fraction (mm)	Weight retained (N)
$d < 0.15$	0	$1.18 < d < 1.25$	6.712
$0.15 < d < 0.25$	0.864	$1.25 < d < 1.4$	4.092
$0.25 < d < 0.425$	1.392	$1.4 < d < 1.7$	0.988
$0.425 < d < 0.6$	1.824	$1.7 < d < 2$	0.332
$0.6 < d < 1$	7.724	$2 < d$	0.284
$1 < d < 1.18$	7.188		

(i) Plot the particle size distribution and % finer versus Φ curves;
(ii) determine d_i and Φ_i for $i = 15.9$, 50, 84.1, and 90 % finer;
(iii) calculate σ_g, d_g, and G; and
(iv) calculate ρ_0, e, ρ_d, and ϕ.

Solution

The particle size distribution curve that is plotted in a semilogarithmic graph representing percentage finer versus sieve size is prepared through following steps. On the graph, the sieve size scale is logarithmic. To find the percentage finer (that is the percentage of sediment passing through each sieve), the percentage retained in each sieve is first obtained as

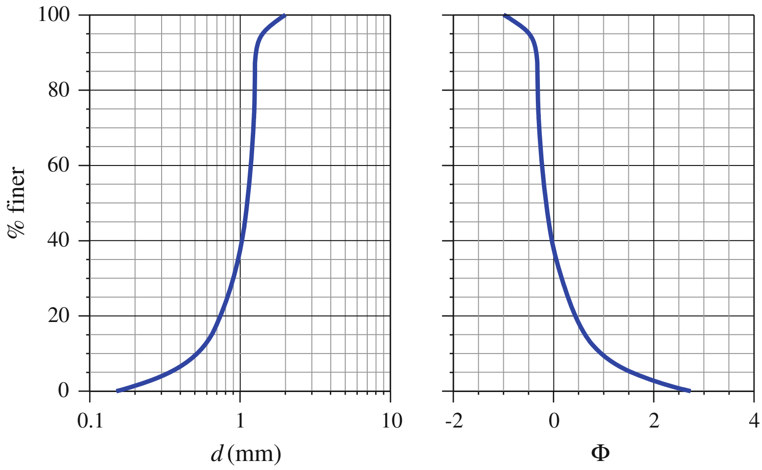

Fig. E1.1 Particle size distribution and % finer versus Φ curves

$$\% \text{ retained} = (\text{weight of sediment retained in the seive} \div \text{total weight}) \times 100\ \%$$

The next step is to determine the cumulative percentage of the sediment retained in each sieve. Thus, the total amount of sediment that is retained in each sieve and the amount in the previous sieves are added. The percentage finer (or the cumulative percentage passing) of the sediment is estimated by subtracting the percentage retained from 100 % as

$$\% \text{ finer} = 100\ \% - \% \text{ cumulative retained}$$

Then, Φ is determined from Eq. (1.18).

(i) The particle size distribution and % finer versus Φ curves obtained from the given sieve analysis are shown in Fig. E1.1.
(ii) From the particle size distribution curve (Fig. E1.1), the following particle sizes d_i and Φ_i corresponding to the given % finer (denoted as fraction i in the form of subscript of d and Φ) are obtained:

$$d_{15.9} = 0.65 \text{ mm}, d_{50} = 1.12 \text{ mm}, d_{84.1} = 1.27 \text{ mm and } d_{90} = 1.36 \text{ mm}$$
$$\Phi_{15.9} = 0.62, \Phi_{50} = -0.16, \Phi_{84.1} = -0.34 \text{ and } \Phi_{90} = -0.44$$

(iii) Using the particle sizes determined in (ii), one can obtain

$$\sigma_g = \left(\frac{1.27}{0.65}\right)^{0.5} = 1.398 \Leftarrow \text{ Eq. (1.14)}$$

$$d_g = (1.27 \times 0.65)^{0.5} = 0.909 \text{ mm} \Leftarrow \text{ Eq. (1.15)}$$

$$G = \frac{1}{2}\left(\frac{1.27}{1.12} + \frac{1.12}{0.65}\right) = 1.429 \Leftarrow \text{ Eq. (1.16)}$$

(iv) Using $d_{50} = 1.12$ mm, one can calculate from Wu and Wang's equation:

$$\rho_0 = 0.13 + \frac{0.21}{(0.002 + 1.12)^{0.21}} = 0.335 \Leftarrow \text{ Eq. (1.21)}$$

$$e = \frac{0.335}{1 - 0.335} = 0.504 \Leftarrow \text{ Eq. (1.22)}$$

$$\rho_d = 2.65 \times 10^3(1 - 0.335) = 1{,}762.25 \text{ kg m}^{-3} \Leftarrow \text{ Eq. (1.23)}$$

To calculate ϕ, the equation given by Zhang et al. is used:

$$\phi = 32.5 + 1.27 \times 1.12 = 33.92^\circ \Leftarrow \text{ Eq. (1.24)}$$

Example 1.2 A sample of 2×10^{-3} m^3 of river water is evaporated to collect suspended sediment of 5.2 N (dry weight), having $d_{50} = 0.1$ mm and $s = 2.65$. Determine C, c, ρ_m, γ_m, and μ_m. Consider μ for a clear water as 10^{-3} Pa s.

Solution

Weight of sediment = 5.2 N; and total volume of water including sediment = 2×10^{-3} m^3
Therefore, one can calculate

$$V_s = \frac{5.2}{\gamma_s} = \frac{5.2}{2.65 \times 9.81 \times 10^3} = 2 \times 10^{-4} \text{ m}^3 \Leftarrow \text{Definition of specific weight}$$

$$V_f + V_s = 2 \times 10^{-3} \text{ m}^3$$

$$C = \frac{2 \times 10^{-4}}{2 \times 10^{-3}} = 0.1 \Leftarrow \text{ Eq. (1.27)}$$

$$c = \frac{2.65 \times 0.1}{1 + (2.65 - 1)0.1} = 0.227 \Leftarrow \text{ Eq. (1.28)}$$

$$\rho_{\rm m} = 10^3 + (2.65 \times 10^3 - 10^3)0.1 = 1{,}165\ \text{kg m}^{-3} \Leftarrow \text{ Eq. (1.29)}$$

$$\gamma_{\rm m} = 1165 \times 9.81 = 11{,}428.65\ \text{N m}^{-3} \Leftarrow \text{ Eq. (1.30)}$$

To calculate $\mu_{\rm m}$, the equation given by Lee is used:

$$\mu_{\rm m} = 10^{-3}(1 - 0.1)^{-(2.5+1.9\times0.1+7.7\times0.1^2)} = 1.34 \times 10^{-3}\ \text{Pa s} \Leftarrow \text{ Eq. (1.33)}$$

Example 1.3 Determine the terminal fall velocity $w_{\rm s}$ in water for a spherical particle with diameter of 5 mm. The relative density of sediment is measured as 2.65. Consider $g = 9.81$ m s^{-2} and υ for a clear water = 10^{-6} m^2 s^{-1}.

Solution

For the nominal diameter $d = 5$ mm, assume a value of $C_{\rm D} = 0.4$. Calculation of $w_{\rm s}$ is as follows:

$$w_{\rm s} = \left[\frac{4}{3} \cdot \frac{(2.65 - 1)9.81 \times 5 \times 10^{-3}}{0.4}\right]^{0.5} = 0.519\ \text{m s}^{-1} \Leftarrow \text{ Eq. (1.34)}$$

Check: For $R_{\rm e}$ (= $w_{\rm s}d/\upsilon = 0.519 \times 5 \times 10^{-3}/10^{-6}$) = 2,595, $C_{\rm D} = 0.43$ is obtained from Fig. 1.5.
For the next trial, consider $C_{\rm D} = 0.43$ and estimate $w_{\rm s}$ again as above. The estimated $w_{\rm s}$ is as 0.5 m s^{-1}.
Check: For $R_{\rm e}$ (= $w_{\rm s}d/\upsilon = 0.5 \times 5 \times 10^{-3}/10^{-6}$) = 2,500, $C_{\rm D} = 0.43$ is obtained from Fig. 1.5. Thus, the assumed and the calculated values of $C_{\rm D}$ are equal.
Therefore, the terminal fall velocity, $w_{\rm s} = 0.5$ m s^{-1}

Example 1.4 A sample of riverbed sand has a nominal diameter of 0.5 mm. The relative density of sediment is measured as 2.65. Find the terminal fall velocity $w_{\rm s}$ using different formulas. Consider $S_{\rm p} = 0.7$, $g = 9.81$ m s^{-2}, and υ for a clear water = 10^{-6} m^2 s^{-1}.

Solution

For the nominal diameter $d_{\rm n} = 0.5$ mm, D_* [= $d_{\rm n}(\Delta g/\upsilon^2)^{1/3}$] is calculated as $D_* = 0.5 \times 10^{-3}\{[(2.65 - 1)9.81]/(10^{-6})^2\}^{1/3} = 12.65$.
Use Eq. (1.40) to determine $w_{\rm s}$ for the values of P, Q, and m given in Table 1.3. The estimated values of $w_{\rm s}$ are furnished in Table 1.5.
From formulas given in Table 1.4 and Eqs. (1.41)–(1.43), following estimations are made:

Table 1.5 Results of w_s

References	P	Q	m	w_s (m s^{-1})
Rubey (1933)	24 (for $d_n \le 1$ mm)	2.1	1	0.0612
Zhang (1961)	34	1.2	1	0.0707
Zanke (1977)	24 (for $d_n \le 1$ mm)	1.1	1	0.0796
Raudkivi (1990)	32	1.2	1	0.0719
Fredsøe and Deigaard (1992)	36	1.4	1	0.0658
Julien (1998)	24	1.5	1	0.0703
Cheng (1997)	32	1	1.5	0.0611
Soulsby (1997)	26.4	1.27	1	0.0737
She et al. (2005)	35	1.56	1	0.0637
Wu and Wang (2006)	53.5 exp($-0.65S_p$)	5.65 exp($-2.5S_p$)	$0.7 + 0.9S_p$	0.0651
Camenen (2007)	24.6	0.96	1.53	0.0664

Hallermeier formula:

$$w_{sc}(3.42 < D_* \le 21.54) = \frac{10^{-6}}{0.5\times10^{-3}}\cdot\frac{12.65^{2.1}}{6} = 0.069\ \text{m s}^{-1}$$

Chang and Liou formula:

$$w_{sc} = 1.68\frac{10^{-6}}{0.5\times10^{-3}}\cdot\frac{12.65^{1.389}}{1 + 30.22\times12.65^{-1.611}} = 0.076\ \text{m s}^{-1}$$

Guo formula:

$$w_{sc} = \frac{10^{-6}}{0.5\times10^{-3}}\cdot\frac{12.65^{3}}{24 + 0.866\times12.65^{1.5}} = 0.064\ \text{m s}^{-1}$$

Dietrich formula:

$$\begin{aligned} w_s &= \frac{10^{-6}}{0.5\times10^{-3}}10^{-1.25572+2.92944\log12.65-0.29445(\log12.65)^2-0.05175(\log12.65)^3+0.01512(\log12.65)^4} \\ &= 0.074\ \text{m s}^{-1} \Leftarrow \text{Eq. (1.41)} \end{aligned}$$

Ahrens formula:

$$\begin{aligned} w_s = \frac{10^{-6}}{0.5\times10^{-3}}\Big\{&0.055\times12.65^3\tanh\left[\frac{12}{12.65^{1.77}}\exp(-4\times10^{-4}\times12.65^3)\right] \\ &+1.06\times12.65^{1.5}\tanh\left[0.016\times12.65^{1.5}\exp\left(-\frac{120}{12.65^3}\right)\right]\Big\} = 0.07\ \text{m s}^{-1} \end{aligned} \Leftarrow \text{Eq. (1.42)}$$

Jiménez and Madsen formula:
For the nominal diameter $d_n = 0.5$ mm, S_* [$= d_n(\Delta g d_n)^{0.5}/\upsilon$] is calculated as $S_* = 0.5\times10^{-3}[(2.65-1)9.81\times0.5\times10^{-3}]^{0.5}/10^{-6} = 44.98$

$$w_s = [(2.65 - 1)9.81 \times 0.5 \times 10^{-3}]^{0.5} \left(0.954 + \frac{20.48}{44.98}\right)^{-1} = 0.064 \text{ m s}^{-1}$$
$$\Leftarrow \text{ Eq. (1.43)}$$

Example 1.4 therefore produces a somewhat varying estimation of terminal fall velocity for a given sediment size, when formulas proposed by different investigators are used.

References

Ahrens JP (2000) The fall-velocity equation. J Waterw Port Coast Ocean Eng 126(2):99–102

Alger GR, Simons DB (1968) Fall velocity of irregular shaped particles. J Hydraul Div 94(3):721–737

Bagnold RA (1954) Experiments on a gravity-free dispersion of large solid spheres in a Newtonian fluid under shear. Proc R Soc London A 255(1160):49–63

Camenen B (2007) Simple and general formula for the settling velocity of particles. J Hydraul Eng 133(2):229–233

Chang H-K, Liou J-C (2001) Discussion of 'The free-velocity equation'. J Waterw Port Coastal Ocean Eng 127(4):250–251

Cheng N-S (1997) Simplified settling velocity formula for sediment particle. J Hydraul Eng 123(2):149–152

Dey S (2003) Incipient motion of bivalve shells on sand beds under flowing water. J Eng Mech 129(2):232–240

Dey S, Sarkar A (2006) Scour downstream of an apron due to submerged horizontal jets. J Hydraul Eng 132(3):246–257

Dietrich WE (1982) Settling velocity of natural particles. Water Resour Res 18(6):1615–1626

Fredsøe J, Deigaard R (1992) Mechanics of coastal sediment transport. World Scientific, Singapore

Goldstein S (1929) The steady flow of viscous fluid past a fixed spherical obstacle at small Reynolds numbers. Proc R Soc London A 123(791):225–235

Guo J (2002) Logarithmic matching and its applications in computational hydraulics and sediment transport. J Hydraul Res 40(5):555–565

Hallermeier RJ (1981) Terminal settling velocity of commonly occurring sand grains. Sedimentology 28(6):859–865

Heywood H (1938) Measurement of the fineness of powdered material. Proc Inst Mech Eng 140(1):257–347

Ippen AT, Eagleson PS (1955) A study of sediment sorting by waves shoaling on a plane beach. Technical Memorandum 63, Beach Erosion Board, United States Army Corps Engineers

Jiménez JA, Madsen OS (2003) A simple formula to estimate settling velocity of natural sediments. J Waterw Port Coast Ocean Eng 129(2):70–78

Julien PY (1998) Erosion and sedimentation, 1st edn. Cambridge University Press, Cambridge

Komura S (1963) Discussion of 'Sediment transportation mechanics: introduction and properties of sediment'. J Hydraul Div 89(1):263–266

Kramer H (1935) Sand mixtures and sand movement in fluvial model. Trans Am Soc Civ Eng 100:798–838

Krumbein WC (1941) Measurement and geological significance of shape and roundness of sedimentary particles. J Sediment Petrol 11(2):64–72

Krumbein WC, Sloss LL (1963) Stratigraphy and sedimentation. Freeman, San Francisco

Lane EW (1947) Report of the subcommittee on sediment terminology. Trans Am Geophys Union 28(6):936–938

Lee DI (1969) The viscosity of concentrated suspensions. Trans Soc Rheol 13(2):273–288

Li Z, Komar PD (1986) Laboratory measurements of pivoting angles for applications to selective entrainment of gravel in current. Sedimentology 33(3):413–423

McNown JS, Lin PN (1952) Sediment concentration and fall velocity. In: Proceedings of the second midwestern conference on fluid mechanics, Ohio State University, Ohio, pp 402–411

Mehta AJ, Lee J, Christensen BA (1980) Fall velocity of shells as coastal sediment. J Hydraul Div 106(11):1727–1744

Oliver DR (1961) The sedimentation of suspensions of closely-sized spherical particles. Chem Eng Sci 15(3–4):230–242

Oseen C (1927) Hydrodynamik. Akademische Verlagsgesellschaft, Leipzig

Raudkivi AJ (1990) Loose boundary hydraulics. Pergamon, New York

Richardson JF, Zaki WN (1954) Sedimentation and fluidisation, part I. Trans Inst Chem Eng 32(1):35–53

Rouse H (1938) Fluid mechanics for hydraulic engineers. Dover, New York

Rubey W (1933) Settling velocities of gravel, sand and silt particles. Am J Sci 225(148):325–338

Schiller L, Naumann A (1933) Über die grundlegen berechnungen bei der schwerkraftaufbereitung. Zeitschrift des Vereines Deutscher Ingenieure 77(12):318–320

Sha YQ (1965) Introduction to sediment dynamics. Industry Press, Beijing

She K, Trim L, Pope D (2005) Fall velocities of natural sediment particles: a simple mathematical presentation of the fall velocity law. J Hydraul Res 43(2):189–195

Soulsby RL (1997) Dynamics of marine sands. Thomas Telford, London

Stokes GG (1851) On the effect of the internal friction of fluids on the motion of pendulums. Trans Cambridge Philos Soc 9:80–85

US Interagency Committee (1957) Some fundamentals of particle size analysis: a study of methods used in measurement and analysis of sediment loads in streams. Report number 12, Subcommittee on Sedimentation, Interagency Committee on Water Resources, St. Anthony Falls Hydraulic Laboratory, Minneapolis, Minnesota

Vanoni VA (1977) Sedimentation engineering. ASCE Manual number 54, American Society of Civil Engineers, New York

Wadell H (1932) Volume, shape and roundness of rock particles. J Geol 40(5):443–451

Wu W, Wang SSY (2006) Formulas for sediment porosity and settling velocity. J Hydraul Eng 132(8):858–862

Zanke U (1977) Berechnung der sinkgeschwindigkeiten von sedimenten. Mitteilungen des Franzius-Instituts für Wasserbau, Technical University, Hannover, Heft 46:230–245

Zhang RJ (1961) River dynamics. Industry Press, Beijing (in Chinese)

Zhang RJ, Xie JH, Wang MF, Huang JT (1989) Dynamics of river sedimentation. Water Power Press, Beijing